Decreased Doublecortin (DCX) immunoreactivity in hippocampus after profound sensorineural hearing loss and vestibular dysfunction in adult mice

Vincent Van Rompaey[1,2] , Alex Liesenborghs[1], Karel Goyvaerts[1], Daan De Herdt[1] , Dorien Verdoodt[1], Marc Lammers[1,2] , Paul Van de Heyning[1,2] , Olivier Vanderveken[1,2] , Krystyna Szewczyk[1] , Sofie Thys[3], Isabel Pintelon[3], Jean Pierre Timmermans[3] , Jordi Llorens[4], Peter De Deyn[5,6,7], Debby Van Dam[5,7]

[1]Deparment of Translational Neurosciences, Faculty of Medicine and Health Sciences, University of Antwerp, Belgium
[2]Department of Otorhinolaryngology & Head and Neck Surgery, Antwerp University Hospital, Belgium.
[3]Core Facility Antwerp Centre for Advanced Microscopy - Laboratory of Cell Biology and Histology, Faculty of Pharmaceutical, Biomedical and Veterinary Sciences, University of Antwerp, Belgium
[4]Departament de Ciències Fisiològiques and Institute of Neurosciences, Universitat de Barcelona, Institut d'Investigació Biomèdica de Bellvitge (IDIBELL), Catalonia, Spain
[5]Laboratory of Neurochemistry and Behaviour, Faculty of Pharmaceutical, Biomedical and Veterinary Sciences, University of Antwerp, Belgium
[6]Department of Neurology, Memory Clinic of Hospital Network Antwerp (ZNA) Middelheim and Hoge Beuken, Antwerp, Belgium
[7]Department of Neurology and Alzheimer Research Center, University of Groningen and University Medical Center Groningen, Groningen, Netherlands

Cite this article as: Van Rompaey V, Liesenborghs A, Goyvaerts K, et al. Decreased Doublecortin (DCX) immunoreactivity in hippocampus after profound sensorineural hearing loss and vestibular dysfunction in adult mice. B-ENT 2021; 17(4): 223-33.

ABSTRACT

Objective: Sensorineural hearing loss (SNHL) and bilateral vestibulopathy (BV) have been associated with cognitive decline and incident dementia. Our aim was to investigate the combined effect of profound SNHL and BV on spatial cognition and hippocampal neurogenesis in adult mice.

Methods: Single oral intake of allylnitrile produces otovestibular failure in less than a week. Behavioral assessment included recording of spontaneous activity, motor activity, spatial cognition, etc. Evaluation of hippocampal neurogenesis was performed 8 weeks after treatment by quantification of neural precursor cells and proliferating cells in the dentate gyrus by staining with doublecortin (Dcx) and Ki67, respectively.

Results: Profound SNHL and BV were confirmed in the allylnitrile-treated mice respectively by means of auditory brainstem response (ABR) and acoustic startle response, and several vestibular tests. Spatial cognitive deficits, i.e. higher latency to target, were observed with the Barnes maze. In the right hemisphere, no statistically significant difference was observed between groups. In the left hemisphere, the difference in mean cell densities of Dcx positive cells was statistically significant when compared to the control group, whereas the difference in mean cell density of Ki67 positive cells did not differ significantly.

Conclusion: Spatial cognitive deficits and decreased immunoreactivity to DCX in the left hippocampus were observed 8 weeks after adult mice acquired profound SNHL and BV.

Keywords: Acquired deafness, auditory perception, cognition, hair cells, hearing

Introduction

Impairment in cognitive performance was demonstrated in several mouse models, since SNHL affects hippocampal neurogenesis and p-tau expression (1-3). The impact of bilateral vestibulopathy (BV) on cognition, however, is less known and frequently overlooked in SNHL patients, while increasing evidence demonstrates its detrimental and irreversible effect on quality of life and work-related disability (4-9). An absent vestibulo-ocular reflex (VOR) results in a loss of steady gaze during head movements, which provokes symptoms such as include imbalance, spatial disorientation and inability to read without stabilizing the head (10, 11). Vestibular dysfunction can be linked to reduced topographical orientation and memory and

has been suggested as a risk factor to AD, due to increased risk of falling and deficits in activities of daily life (ADL) (12).

Evidence suggests that different areas in the hippocampus, active in cognitive domains such as spatial and non-spatial learning and memory, are indeed involved in processing hearing and balance cues and are affected by sensory loss (13-24). New neurons in the adult hippocampus originate in progenitor cells located at the border between the hilus and granular cell layer, which is a region referred to as the subgranular zone (SGZ) of the dentate gyrus (DG) (25).

Nitriles are increasingly used in the chemical industry and are known for their toxic effects including acute lethality, osteolathyrism and neurotoxicity. This neurotoxic potential was first revealed by the behavioral effects of 3,3'-iminodipropionitrile (IDPN) in rodent species, and later established in other nitriles, such as allylnitrile (3-butenenitrile) (26-30). However, data from rat studies indicated that the behavioral effects could in fact be explained by vestibular sensory hair cell loss, similar to lesions induced by chemical or surgical ablation (30-34).

The objective of this study was to investigate the effect of profound SNHL and BV on behavioral spatial cognition and hippocampal neurogenesis in adult mice. To study onset and irreversible otovestibular failure, we used the allylnitrile toxicity mouse model in a 129S background, which has been established to provide a selective hair cell degeneration, days after oral intake. Our hypothesis was that acquired otovestibular failure has a negative effect on spatial navigation and hippocampal neurogenesis.

Methods

Animals
All procedures were approved by the animal ethics committee of the University of Antwerp (reference number 2017-51) and were compliant to the European Communities Council Directive on the protection of animals used for scientific purposes (2010/63/EU).

We evaluated 129S1/SvImJ mice, a strain that is known for significant variability per substrain: from resistant to noise up to increased progression of age-related sensorineural hearing loss. (35) Because sex differences have been observed in nitrile metabolism and toxicity in mice, we only used males (36, 37).

The mice were housed four-five per cage in standard type III plastic cages. Cages were stored in sound-proof rooms at con-

Main Points:

· Sensorineural hearing loss and bilateral vestibulopathy have each been associated with cognitive decline.
· Oral treatment with allylnitrile produces profound sensorineural hearing loss and vestibular deficit in mice.
· Spatial cognitive deficits were observed in allylnitrile-treated mice using the Barnes maze test.
· Decreased neurogenesis was observed in the left hippocampus.
· Reduction of hippocampal neurogenesis due to otovestibular failure may induce cognitive deficits 8 weeks after onset in mice.

stant room temperature (20-24°C) and humidity (45%). The animals were maintained on a 12 h/12 h light–dark cycle. Sample sizes were based on Mead's resource equation (38).

Chemicals and dosing
A single dose of allylnitrile (3-butenenitrile) was administered by awake oral gavage in 6 ml/kg of corn oil at 1 mmol/kg. To reduce systemic toxicity without reducing otovestibular toxicity due to hair cell loss, trans-1,2-dichloroethylene (98 %) (TDCE) was administered intraperitoneally (i.p.) at 100 mg/kg in 6 ml/kg of corn oil 30 min before and 6 and 24 hours after administration of allylnitrile (34). The acute lethality that characterizes many nitriles, including allylnitrile, is mainly due to the release of cyanide in the body through metabolization by the alcohol/acetone-inducible isoform of the P450 cytochrome CYP2E1. CYP2E1 can be pharmacologically inhibited by TDCE, thereby limiting the acute toxicity of allylnitrile, but leaving the vestibular and cochlear toxicity unchanged. The animals were observed daily for 3–4 days and at least twice a week afterwards and rated for overall toxicity. The animals were euthanized if they met the criteria of the ethical limits of suffering.

Chronology of procedures
The mice arrived at the lab at 8 weeks of age. After at least 1 week of acclimatization, baseline audiovestibular evaluation was carried out. Allylnitrile and TDCE co-treatment was performed at 16 weeks of age. In the following 8 weeks after exposure to allylnitrile, the mice were evaluated for hearing (auditory brainstem responses and acoustic startle response) and vestibular function (behavioral vestibular tests). At 24 weeks of age, mice were euthanized for neuroanatomical study of the brain.

Hearing evaluation

Auditory Brainstem Response (ABR) testing was performed to evaluate auditory function: Prior to ABR recordings, animals were anesthetized using isoflurane and positioned on a homeothermic heating blanket inside a sound attenuating chamber. All ABR recordings were performed under free-field conditions using a single loudspeaker which was positioned 10 cm opposite to the rostrum of the animals. Mice were exposed to tone bursts of 2 ms length, with a gate of 1 ms, at frequencies of 2, 4, 8, 16 and 32 kHz, in 5 dB steps starting at 80 dB SPL (decibel of sound pressure level) down to a minimum SPL of 10 dB at 32 stimuli per second**,** this with a mean of 800 trials per frequency and per dB SPL. The ABR threshold we used, was the lowest stimulus with a visual detectable waveform.

Acoustic startle response. The acoustic startle response was determined at 120 dB using standard startle boxes (Kinder Scientific, USA) with a few modifications (39).

Evaluation of vestibular function and motor function

Vestibular dysfunction rating (VDR): Disturbance of vestibular function was determined using a battery of behavioral tests to evaluate the bilateral symmetrical loss that occurs following systemic exposure to ototoxic nitriles (31, 32, 40), including three measures of spontaneous motor behaviour and three vestibular reflexes, each rated 0 (normal behaviour) to 4 (max-

imal deficit in behaviour). The mice were placed in an open arena for 1 min (cage type III H) and rated by animals circling, retropulsion, and abnormal head movements (head bobbing), and subsequently also by the tail-hang reflex, contact inhibition of the righting reflex, and air-righting reflex tests. A higher score is associated with more profound vestibular dysfunction. In addition, animals were observed for signs of asymmetry in the vestibular damage (41, 42). Unilateral vestibular damage causes animals to tilt their heads to the side. In the tail-hang test, unilateral lesions cause body rotation around the tail axis rather than ventral bending.

Additionally the wire suspension test, stationary beam test and accelerating rotarod were performed to corroborate VDR findings.

Gait analysis: Gait characteristics (stride length, toe span, and track width) were analyzed by applying ink to the hind paws of animals. Mice were then allowed to walk on a strip of paper in a brightly lit walk lane (width: 4.5 cm; length: 40 cm), towards a dark goal box. At least two complete gait patterns from each mouse were obtained.

Evaluation of activity patterns and open field behavior

Circadian home cage ambulatory activity patterns: Using 3 infrared sensors, the number of beam interruptions was recorded over a 47-hour period in 30-min bins, keeping into account that the initial hours that the mouse is placed in this new environment are to be considered as exploration. Recordings started at 4:00 PM on day 1 and ended at 3:00 PM on day 3.

Open field (OF) behavior: A computerized video tracking system (Noldus EthoVision® XT, Noldus, Wageningen, The Netherlands) was used to record trajectories and calculate path length and number of entries in the centre circle or the 7 cm x 7 cm corners of the open field. Exploring the centre area of this field, rather than staying in the corner, is a measure for anxiolytic and increased exploratory behavior.

Behavioral analysis of cognitive function

Novel object recognition (NOR): To assess hippocampal-dependent learning and memory, a NOR test was performed. On the first two days (habituation phase) each animal was introduced into the empty NOR setup (20 cm × 40 cm; length × width) for 10 minutes. On day 3 (familiarization phase), two identical objects were placed into the NOR setup and the animals were again allowed to freely explore the cage for 10 min. During the test phase on day 4, one object was replaced with a new object different in color and shape, and the animals were again recorded for 10 minutes. The novel object in the testing phase was placed left or right (50%) to account for confounding spatial cues. All movements were tracked and processed using Noldus EthoVision® XT software (Noldus, Wageningen, The Netherlands). Exploration time was defined as the time during which the nose-point of the animal was directed towards one of the objects within proximity of 3 cm. The preference index (PI) was calculated as the time spent exploring the novel object divided by the total time exploring both objects. The discrimination index (DI) was defined as the time near the novel object minus the time near the familiar object divided by the total exploration time.

Barnes maze: The Barnes maze assesses hippocampus-dependent visual-spatial learning and memory. The setup consisted of the circular maze (diameter 100 cm) in white acrylic plastic with 20 holes (diameter 5 cm) along the edge of the maze. One of the holes gives access to an escape goal box, of which the location of the escape box is semi-randomized over the test population. The maze is surrounded by invariable visual extra-maze cues. During an initial adaptation trial, the mouse was placed in the center of the maze under a starting box for 15 seconds. Upon removal of the starting box, the mouse was gently guided towards the goal box where it had to remain for 2 minutes. The first experimental trial starts immediately after this adaptation trial. Each mouse was trained during four daily trials (inter-trial interval 15 minutes) for 4 consecutive days. A trial ended when the escape box is found or after 3 min after which the animal was guided towards the goal box. Probe trials (90 seconds) in which the goal box was replaced by a dummy box investigated memory retention at day 5 and day 12. Animals' trajectories were recorded using Noldus EthoVision® XT software (Noldus, Wageningen, The Netherlands).

Histological analysis of neurogenesis

After completion of behavioral testing, the anaesthetized animals (0.3 ml/mouse Nembutal) were dissected. Both brain hemispheres were fixated to acquire coronal vibratome slices (100 μm). For each animal, slices were evaluated under a stereomicroscope to determine the first slice were the dentate gyrus was clearly visible. For each animal, ≤ 6 slices were used for immunostaining. Ki-67, an endogenous marker for proliferating cells, is a reliable marker for neurogenesis in the adult brain since it is expressed during mitosis and has a short half-life. In addition, Ki-67 can be detected easily by immunohistochemistry. Doublecortin (Dcx) is a microtubule-associated phospho-protein required for neuronal migration and differentiation that is expressed in migrating neurons during the development of the central nervous system. Dcx expression is believed to be specific to newly generated neurons because virtually all Dcx-positive cells express early neuronal antigens. Therefore, Dcx may be a good marker for immature progenitor cells in neurogenesis of the adult brain (25). Slices were stained with Dcx and Ki-67 to prepare for microscopic imaging. For each animal, 6 slices were imaged using the Nikon HTM, according to a standardized imaging protocol. Evaluation of neurogenesis in the hippocampal dentate gyrus was performed by quantification of neural precursor cells, immunopositive for Dcx, and proliferating cells which were immunopositive for Ki67. For each animal, 6 slices of the left and right hemisphere were analyzed, in the rostral-caudal axis with 200 μm intervals between slices. For each slice, cells in the subgranular zone (SGZ) of the dentate gyrus, immunopositive for Dcx or Ki67, were manually counted through the complete thickness of the Z-stack (60 μm) by an observer blinded to the identity of the sample. The analysis of the right and left hemispheres was performed by different observers. The length of the SGZ was measured using polyline. For every slice, the number of cell profiles (Dcx or Ki67-positive) was divided by the length of the SGZ to obtain cell density.

Statistical analysis

Pre and post ABR measurements were compared using a non-parametric Wilcoxon signed-rank test, since assumptions

Table 1. ABR thresholds at each frequency per treatment group before (baseline) and after treatment

Baseline		ABR threshold (dB SPL)				Mann-Whitney U		
Frequency	Treatment		N	Mean	SD	U	Z	Sig. (2-tailed)
8 kHz	Control		11	77.27	8.76	50.50	-1.060	0.289
	Allyl nitrile + TDCE		12	80.83	7.02			
16 kHz	Control		11	61.81	8.45	45.00	-1.325	0.185
	Allyl nitrile + TDCE		12	65.83	5.15			
32 kHz	Control		11	84.55	1.51	65.50	-0.063	0.950
	Allyl nitrile + TDCE		12	84.58	1.44			
After treatment		**ABR threshold (dB SPL)**				**Mann-Whitney U**		
Frequency	Treatment		N	Mean	SD	U	Z	Sig. (2-tailed)
8 kHz	Control		11	73.64	12.27	30.00	-2.870	0.004*
	Allyl nitrile + TDCE		12	85.00	0.00			
16 kHz	Control		11	66.82	11.46	6.00	-4.085	< 0.001*
	Allyl nitrile + TDCE		12	85.00	0.00			
32 kHz	Control		11	84.09	3.02	60.00	-1.044	0.296
	Allyl nitrile + TDCE		12	85.00	0.00			

Mann-Whitney U test was carried out to compare the treatment groups.
* presents a statistically significant difference (p < 0.05).
ABR, auditory brain stem response; TDCE, trans-1,2-dichloroethylene; SD, standard deviation; SPL, sound pressure level
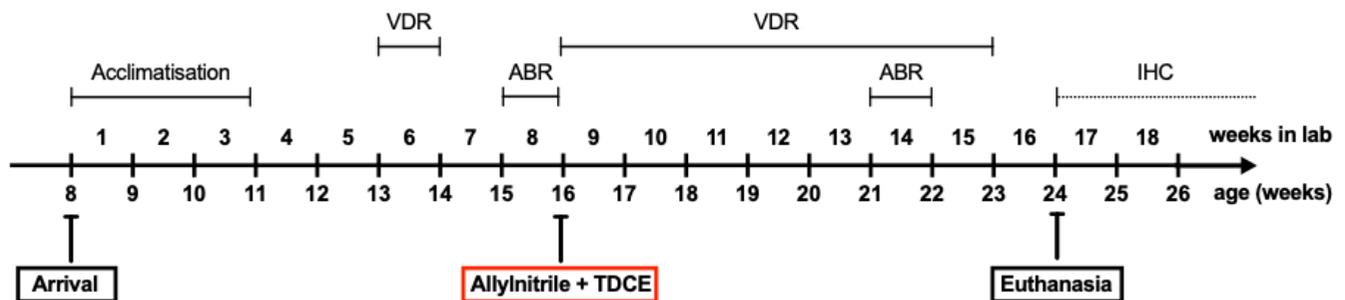
Figure 1. Auditory brain stem response (ABR) thresholds at baseline (left panel) and after treatment (right panel) for each treatment group. Data are represented as mean with standard deviation. *, statistically significant difference (p<0.05) between treatment groups. TDCE, trans-1,2-dichloroethylene.

of normality were not met (according to the Shapiro–Wilk test of normality). For the same reason, a Mann-Whitney-test was used for comparing ABR results between treatment groups for each frequency. Since not all VDR-data were normally distributed, a non-parametric Friedman test per treatment group was computed to identify treatment effects over time. If a significant effect was found, Dunn-Bonferroni post-hoc analysis was carried out to identify which specific VDR results were significantly different over time. To analyze immunohistochemistry data, we used for each hemisphere an independent T-test to compare control versus treatment group. Before analysis, assumptions were confirmed. All data are represented as mean (M) ± standard deviation (SD). Statistical analyses were computed using IBM SPSS Statistics for Windows, Version 26.0 (IBM Corp. Armonk, New York, USA). GraphPad Prism 8.0.2 (GraphPad Software (San Diego, California, USA) was used for the generation of graphs.

Results

Weight and health condition

No mortality was observed after 1 mmol/kg of allylnitrile with TDCE co-treatment. Animals that received 1 mmol/kg of allylnitrile experienced a maximal weight loss of 12.8% at day 2 after dosing.

Hearing evaluation

Auditory brainstem recording: All mice underwent ABR (table 1 and figure 1): twelve animals were treated with allylnitrile + TDCE and 11 control mice were treated with corn oil. To evaluate hearing loss associated with allylnitrile intoxication, ABR thresholds were evaluated at two timepoints: 1 week before allylnitrile intoxication (baseline) and 6 weeks after allylnitrile intoxication. When no ABR pattern was observed at the highest intensity of 80 dB tested, the threshold was set at 85 dB,

meaning profound sensorineural hearing loss or deafness for that frequency. In the control group (n = 11), no significant differences were found in ABR thresholds at any frequency before and after treatment. At baseline, no statistically significant difference in ABR thresholds was observed at any frequency between the two treatment groups. A statistically significance between the treatment and control group was found at 8 kHz (U = 30.000; Z = -2.870; p = 0.004) and 16kHz (U = 6.000; Z =-4.085; p < 0.001) after treatment.

Acoustic startle. No statistically significant differences were observed at baseline between both groups: 1.1375 N (allylnitrile) and 1.0445 N (control), p = 0.477 (Mann Whitney test; two-tailed P-value). The acoustic startle response after treatment in allylnitrile mice was 0.0575 N versus 0.8682 N in the control group, with a statistically significant difference, p<0.0001 (Mann Whitney test; two-tailed P-value). No acoustic startle was observed at 120 dB in mice exposed to allylnitrile + TDCE. Results can be found in Appendix 4.

Evaluation of vestibular and motor function
Baseline vestibular evaluation was performed 2 weeks prior to treatment. Post-treatment evaluation was carried out up to 55 days after exposure. Individual VDR scores are plotted in figure 2 (left panel). The VDR score of one mouse in the treatment group recovered quickly after the administration of allylnitrile. After excluding the data of this animal, mean VDR scores per treatment group were calculated (figure 2, right panel). The mean VDR score of the control group remained 0 throughout follow-up, which represents normal vestibular function. The allylnitrile and TDCE co-treatment resulted in mean total vestibular rating scores of 13.55 ± 1.13 at 4 days after exposure and 12.55 ± 1.75 at 55 days after exposure (figure 2, right panel), which represents a deterioration of vestibular function in this group. In the allylnitrile-exposed group, the VDR results were significantly different over time ($\chi^2(10)$ = 53.63; p<0.001, non-parametric Friedman test). Dunn-Bonferroni post-hoc tests were carried out revealing significant differences between the VDR results at baseline and 4 days (p = 0.046), 5 days (p < 0.001), 6 days (p < 0.001), 8 days (p < 0.001), 10 days (p < 0.001) and 48 days (p = 0.022) after treatment. Further pairwise comparisons did not show any significant differences. In the control group, the Friedman test did not show a significant difference ($\chi^2(10)$ = 0.00; p = 1.000). To compare VDR results between treatment groups, we calculated a Mann-Whitney U test at each point in time. At baseline, no significant difference in VDR scores was observed between the treatment groups. After treatment, VDR scores were significantly different at each point in time.

A higher number of falls was observed in the allylnitrile-treated mice when performing the wire suspension (p = 0.0013) and stationary beam test (p < 0.001). While performing the rotarod, 5 out of 11 allylnitrile-treated mice had to be disqualified because they were unable to perform the test. Nevertheless, statistically significant deterioration in rotarod performance was observed in the remaining 6 allylnitrile-treated mice (p = 0.004). Significantly increased track width was observed in allylnitrile-treated mice during gait analysis typical for mice with balance-related symptomatology (p < 0.001). Data can be found in supplemental appendix 1.
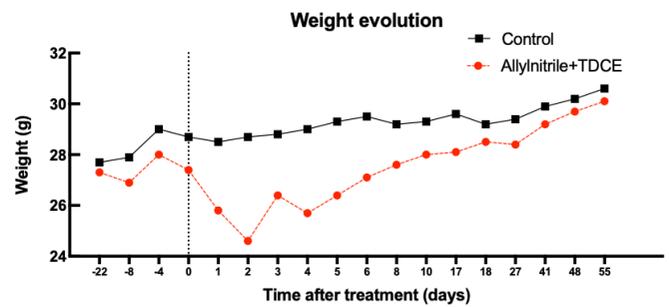
Figure 2. Vestibular dysfunction rating (VDR) scores. Individual VDR scores per mouse (left panel) and mean VDR scores with standard deviation (right panel) are shown. The dotted line represents the VDR score of one mouse which recovered after allylnitrile exposure. Mann-Whitney U tests were carried out to compare treatment groups at each point in time. *, statistically significant difference (p< 0.05) between treatment groups. TDCE, trans-1,2-dichloroethylene.

Evaluation of activity patterns and open field behavior
We observed general differences in circadian home cage ambulatory activity patterns between treatment groups with increased activity in allylnitrile-treated animals (figure 3). Interaction indicates genotype-dependent differences in particular time frames (p < 0.001). No statistically significant differences were observed in open field exploration prior to treatment. Allylnitrile-treated mice were observed to travel a significantly longer distance (related to higher velocity) than sham-treated mice (p < 0.001), while there is no overall difference in exploration pattern. Data can be found in supplemental appendix 2.

### Novel object recognition and Barnes maze
No statistically significant preferences for left/right or cognition-related parameters of novel object recognition were observed between the sham and allylnitrile group, except for total distance travelled (which was increased in the allylnitrile-treated mice, p = 0.023). While performing the Barnes maze test increased latency to target (p = 0.009) and increased total latency (p = 0.016) were observed (figure 4). Data can be found in supplemental appendix 3.

### Histological analysis of neurogenesis
Before statistical analysis, the average cell densities of Dcx- and Ki67-positive cells per mouse were calculated to prevent pseudo-replication of data. Cell densities are expressed in cell count of Dcx- and Ki67-positive cells per length (µm) of the SGZ. To compare mean cell densities between control and treated mice, we used an independent T-test. Assumptions of normality and homogeneity of variances were met.

We excluded data from two mice: one because of premature mortality and one because of recuperation of vestibular function after treatment with allylnitrile. In addition, we had to exclude data from four mice because of inadequate immunohistochemistry of the left hemisphere. Consequently, we analyzed data from 22 mice (11 control, 11 treatment) for the right hemisphere and data from 18 mice (9 control, 9 treatment) for the left and both hemispheres.

Right hippocampus: The difference in mean cell density of Dcx-positive cells between the control group (M = 0.015; SD = 0.004) and the treated group (M = 0.014; SD = 0.005) was not
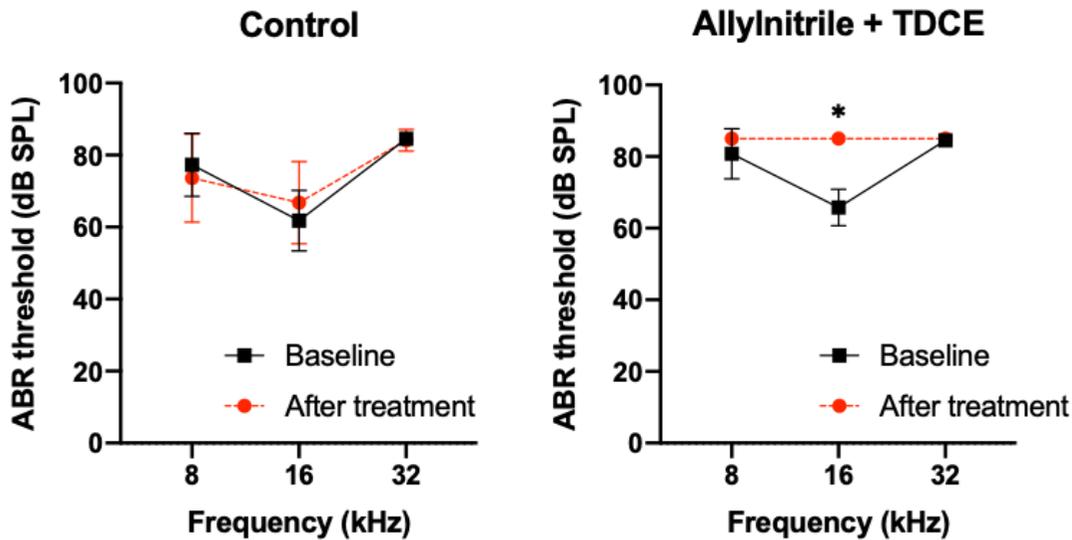
Figure 3. Circadian home cage ambulatory activity patterns. Cages were placed in an enclosure equipped with ventilation to maintain optimum ambient temperature and illumination to simulate the light/dark cycle of the mice. The number of beam interruptions was recorded over a 47-hour period in 30-min bins. Recordings started at 16.00 h on day 1 and ended at 15.00 h on day 3. Increased activity can be observed in the group of animals treated with allylnitrile.
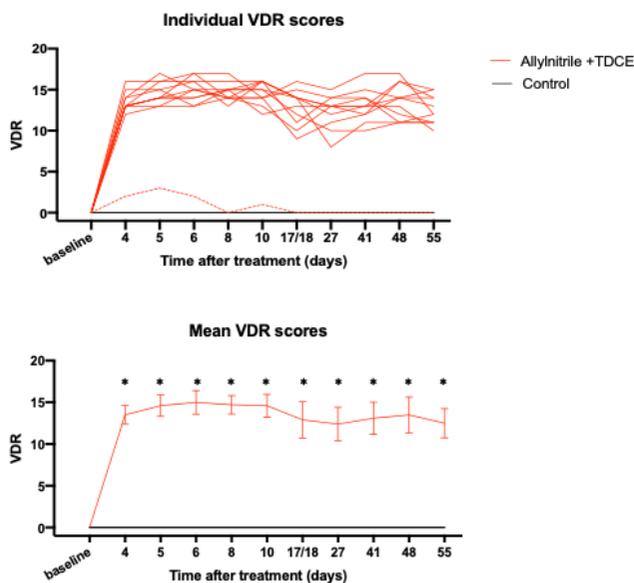
Figure 4. Total latency and latency to target during the Barnes maze test. Animals' trajectories were recorded using Noldus EthoVision® XT software (Noldus, Wageningen, The Netherlands). Statistically significant differences can be observed when comparing the allylnitrile-treated group with the control group.

significant (t(20) = 0,532; p = 0.600). The difference in mean cell density of Ki67-positive cells between control group (M = 0.010; SD = 0.003) and treated group (M = 0.009; SD = 0.003 was not significant (t(20) = 0.876; p = 0.392). Results can be observed in table 2 and figure 5 (left panel).

Left hippocampus: The difference in mean cell density of Dcx-positive cells between the control group (M = 0.019; SD = 0.006) and the treated group (M = 0.013; SD = 0.005) was significant (t(16) = 2.378; p = 0.030). The difference in mean cell density of Ki67-positive cells between the control group

(M = 0.009; SD = 0.004) and the treated group (M = 0.007; SD = 0.003) was not significant (t(16) = 1.243; p = 0.232). Results can be observed in table 2 and figure 5 (right panel).

Both hemispheres: We did not pool data of the left and right hemispheres to calculate mean cell-densities per mouse since observations were made at two different time points. For the same reason, we did not compare the different cell densities between the left and right hemispheres.

Discussion

In this study we were able to induce otovestibular loss (i.e. BV and profound SNHL) in adult 129S mice. We observed a significant decrease in the number of neural precursor cells (identified by Dcx immunohistochemistry) in the dentate gyrus of the left hippocampus 8 weeks after onset. We also observed impaired spatial cognition when evaluating mice with the Barnes maze.

Model for bilateral otovestibular failure
A mouse model with established selective symmetrical otovestibular failure, days after allylnitrile administration, was used. The effects of allylnitrile on audiological and vestibular function are well described in literature (26-30, 32). As expected, we confirmed otovestibular dysfunction following allylnitrile exposure. The acute toxicity of allylnitrile could lead to mortality, due to cyanide release from the parent nitriles after metabolisation by the 2E1 isoform of cytochrome P450 (CYP2E1), as demonstrated by decreased mortality in CYP2E1-null mice (43). In our study, no systemic toxicity was observed after co-treatment of TDCE, a CYP2E1-inhibitor as no humane endpoints were reached during this study that were indicative of reduced animal welfare and required premature removal of animals from the study. (34).

ABR analysis did not yield any significant difference in ABR thresholds over time in the control group across all frequen-
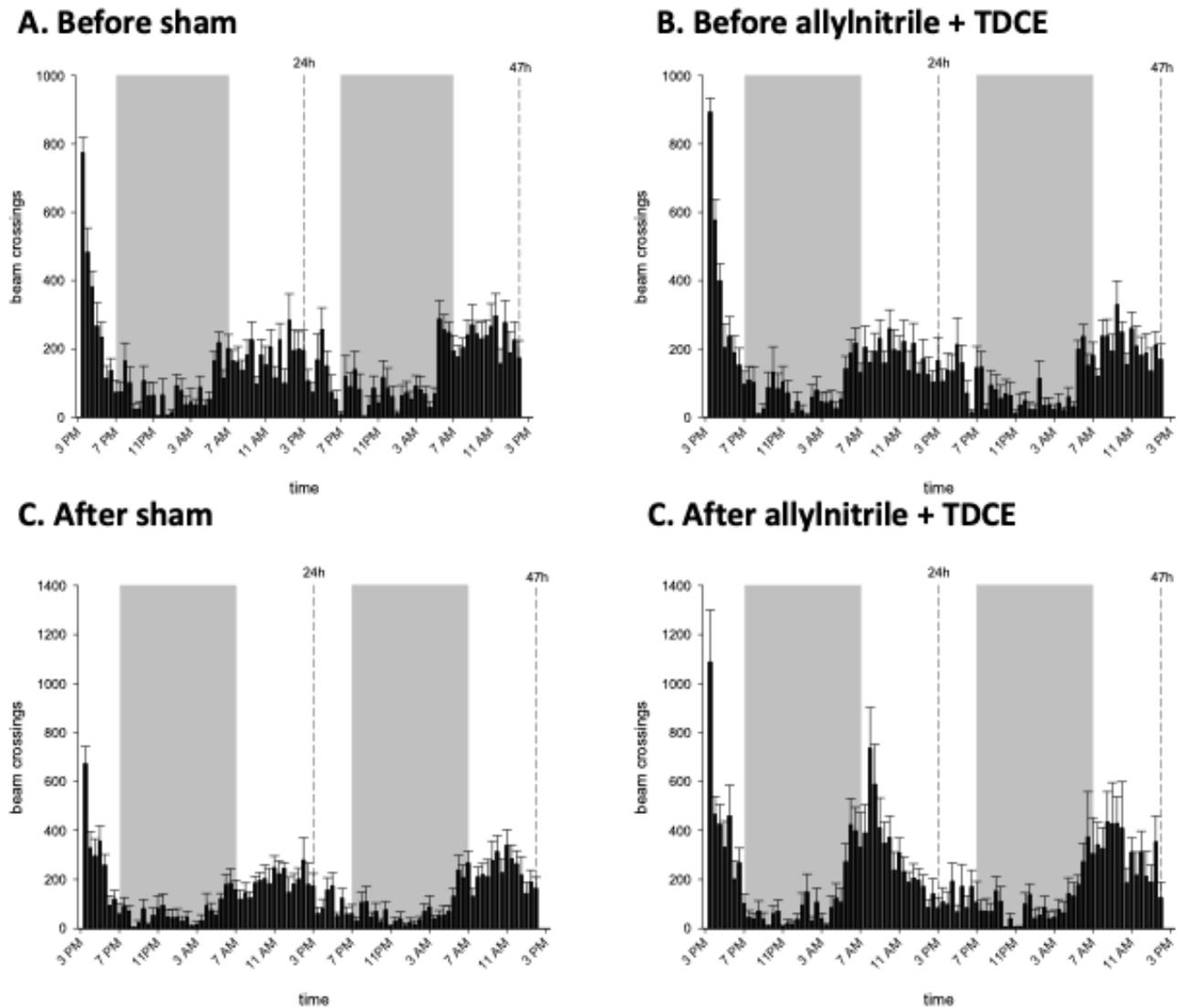
Figure 5. Quantitative analysis of neurogenesis in the right and left hippocampus, based on immunohistochemical stainings for doublecortin (DCX) and Ki-67. Data are represented as mean with standard deviation. No significant differences were found between the treatment groups.

cies. Within the treatment group a significant elevation in ABR threshold was found at 16 kHz, while no difference was observed at 8 and 32 kHz. A possible explanation could be hearing loss prior to treatment, known to occur in the 129S strain. Because the highest intensity tested in the ABR test was 80 dB SPL, the threshold over this level was assigned as 85 dB SPL. This ceiling effect was likely to cause an underestimation of the threshold in the allylnitrile-exposed group. VDR scores were more in our line of expectation. The rating scores for the control group remained 0 throughout the study, which represents normal vestibular function. The score for the treatment group, which started at 0, rose to a score of 13.55 ± 1.13 within 4 days after allylnitrile + TDCE administration. This score remained consistent for the duration of the study, with the last test performed 55 days after treatment. Remarkably, one mouse recovered back to baseline vestibular function within 8 days and was removed from the analysis.

Although complete deafness was observed after treatment with allylnitrile (and confirmed with the acoustic startle re-

sponse measurements), we also observed significant pre-treatment hearing loss. This could be explained by noise-induced hearing loss due to the transportation of the mice or by the use of isoflurane as an anaesthetic gas. Previous research suggests that the use of isoflurane in mice has a negative impact on hearing function by interference with synaptic vesicle release, determined by ABR thresholds, across all frequencies compared with, for example, ketamine/xylazine anaesthesia. (44-51) In contrast, Kim et al. (52) observed higher DPOAE thresholds in mice anesthetized with isoflurane, but no difference in ABR thresholds compared to mice anesthetized with ketamine/xylazine.

Quantitative analysis of neurogenesis in the hippocampus
The negative impact of SNHL on cognitive function is well described in literature (4-9, 53, 54). Multiple studies in humans have provided proof of a significant correlation between hearing loss on the one hand and age-related cognitive decline and incidence of dementia on the other hand. (3, 55-59).

Table 2. Quantitative analysis of neurogenesis in the right and left hippocampus on the basis of immunohistochemical stainings for DCX and Ki-67

Right hippocampus	Cell densities (cell count/μm)				Independent t-test		
Staining	Treatment	N	Mean	SD	t	df	Sig. (2-tailed)
DCX	Control	11	0.015	0.004	0.532	20	0.600
	Allyl nitrile + TDCE	11	0.014	0.005			
Ki-67	Control	11	0.010	0.003	0.876	20	0.392
	Allyl nitrile + TDCE	11	0.009	0.003			
Left hippocampus	Cell densities (cell count/μm)				Independent t-test		
Staining	Treatment	N	Mean	SD	t	df	Sig. (2-tailed)
DCX	Control	9	0.019	0.006	2.378	16	0.030*
	Allyl nitrile + TDCE	9	0.013	0.005			
Ki-67	Control	9	0.009	0.004	1.243	16	0.232
	Allyl nitrile + TDCE	9	0.007	0.003			

Independent t-tests were carried out.
DCX, doublecortin; TDCE, trans-1,2-dichloroethylene; SD, standard deviation

In humans, an important role has been suggested for the hippocampus is suggested as a neuro-biological correlate for cognitive decline in patients with hearing loss. In these MRI studies, a relationship between hearing loss on the one hand and decreased brain volume, including temporal lobe and hippocampal volume, on the other hand was observed. (60-62) A potential mechanism involved in hippocampal atrophy is decreased hippocampal neurogenesis. Ongoing decreased adult hippocampal neurogenesis, as a result of decreased auditory input, will subsequently lead to impairment of learning and memory. This mechanism lends support to a bottom-up causality and is further substantiated by evidence from rodent studies. Yu et al. (63) demonstrated hippocampal synaptic changes and reduced spatial memory in C57BL/6J mice with age-related hearing loss, as indicated in a Morris water maze tesy. Also, noise-induced hearing loss is associated with impaired hippocampal neurogenesis and reduced performance at spatial memory tasks in mice (1, 2, 24). Kraus et al. (24) and Liu et al. (1), just like us, both used Ki 67 and Doublecortin immunohistochemistry of the dentate gyrus to quantify the hippocampal neurogenesis. Both studies reported a significant negative effect of noise exposure on both the Dcx and Ki 67 cell counts, compared to sham controls. Freemyer et al. (64) were even able to detect a decrease in hippocampal neurogenesis as early as 1 month after unilateral sound damage. A recent study in rats demonstrated that local field potentials (LFPs) can be evoked in the hippocampus by selectively stimulating the cochlea electrically (65). All these observations may be instrumental in understanding how maladaptive hippocampal neuroplasticity can be caused in response to tinnitus and peripheral vestibular disorders.

Apart from the impact of SNHL on cognitive function, vestibular impairment is known to reduce cognitive functions as well, more specifically - but not only - spatial cognition. Brandt et al. (19) published an important study on this subject in patients with neurofibromatosis type 2, who underwent bilateral vestibular nerve section; they observed significantly decreased spatial navigation skills and reduced hippocampal volumes

(measured with MRI) compared to a control group. We were able to observe impairment of spatial cognition in our study by means of the Barnes maze test. This impairment may be related directly to BV or indirectly via reduced hippocampal neurogenesis. The Barnes maze, particularly the acquisition phase followed by the acquisition probe trial, allows an evaluation of spatial learning and spatial memory, believed to be associated with hippocampus function (66). It has been reported as less stressful for animals (especially mice) than the Morris water maze, because there is no water immersion and is not so physically demanding for the animals (67).

The degree of atrophy correlated with the degree of impairment in spatial memory (19). These observations were supported by several studies demonstrating a decrease in grey matter in the hippocampal region in humans (20, 23), although only partial bilateral vestibular impairment was observed. Thereby, hippocampal atrophy is a potential neuroanatomic correlate of decreased spatial cognitive ability associated with vestibular impairment (68). However, it should be pointed out that these studies did not correct for hearing impairment. Dobbels et al. (69-71) studied the effect of hearing loss and vestibular loss on cognitive impairment in patients with bilaterally reduced vestibular function. Both vestibular and hearing dysfunction were associated with different subscales of the cognitive test battery they used. These findings suggest that, similarly to the impact of hearing loss on cognitive function, the sensory deprivation hypothesis may also apply to the relationship between vestibular function and cognition.

In contrast to the observed impact of hearing loss on hippocampal neurogenesis, to our knowledge, hippocampal atrophy following bilateral vestibular dysfunction has not been reported in animal studies (72, 73). Zheng et al. (73) reported no significant differences in hippocampal neuronal number or volume compared to controls 16 months after bilateral vestibular deafferentation (BVD), although these animals showed severe spatial memory deficits. In contrast, using bromodeoxyuridine (BrdU) as a marker of cell proliferation, they found

that the number of BrdU-labeled cells significantly increased in the dentate gyrus of the hippocampus between 48h and 1 week following BVD. These results suggest a dissociation between the effects of BVD on spatial memory and hippocampal structure in rats and humans, which cannot be explained by an injury-induced increase in cell proliferation. In later published data, Balabhadrapatruni et al. (74), in a later study, observed more subtle morphological changes in the rat hippocampus following vestibular loss. Using Golgi staining, they detected alterations in dendritic intersections, i.e. a significant decrease in basal but not apical dendritic intersections was seen in the CA1 region of the hippocampus compared to sham animals at 1 month after BVD (74).

Our results show a decrease in cell density of neuronal Dcx-labelled precursor cells, within 8 weeks after loss of otovestibular input, as a marker for hippocampal neurogenesis in the left hippocampus compared with sham controls. In contrast, the cell-densities of Ki67-labeled proliferating cells in the dentate gyrus were not significantly different between the two treatment groups. It is currently not clear if the decline in the number of differentiated adult neural progenitors is the result of an effect on the rate of conversion of proliferative cells into immature neurons, or whether it is caused by changes in the survival rate of the immature neurons.

In humans, there tends to be a left-to-right difference in hippocampal volume (75). Numerous studies have reported a smaller hippocampal volume in Alzheimer's disease (AD) compared to control patients and hippocampal atrophy is as a consistent finding in AD. In their meta-analysis of MRI-studies in patients with mild cognitive impairment (MCI) or AD, Shi et al. (75) found significant bilateral hippocampal atrophy in both MCI and AD patients. Also, a left-less-than-right asymmetry was found in all three groups (AD, MCI, control). In patients with unilateral vestibular neuritis in their medical history, zu Eulenburg et al. (76) found hippocampal atrophy on the left side irrespective of the side of vestibular failure. Kremmyda et al. (20) performed an MRI-data analysis of patients with BV and equally found a left-more-than right hippocampal atrophy as well. (20)

Our data suggest that the left hippocampus may be prone to decreased hippocampal neurogenesis, which could (at least partly) explain the left-to-right difference observed in humans. However, our observations are in contrast with results of Kraus et al. (24), who did not observe any difference in Dcx-labelled cell counts between the left and the right hippocampus in any of the treatment groups (noise-induced hearing loss compared to sham controls) at 10 weeks after unilateral noise-induced hearing loss in rats.

Limitations
Data from 22 male mice for the right hemisphere and data from 18 mice for the left hemisphere were analyzed. Allgoewer et al. (77) calculated the necessary sample size in animal experiments using a Markov Chain Monte Carlo approach. Animal experiments with continuous outcome parameters should have six animals in each group to have sufficient statistical power, which is a lower number than our number of mice.

Furthermore, for one-way ANOVA, another power analysis for animal studies, the number of animals in each group should be

between six and eleven (38), which is in line with our number of mice. In conclusion, the number of mice used in our experiments is sufficient for statistical significance according to multiple calculation methods for power analysis.

To the best of our knowledge, no studies have been performed addressing the potential of allylnitrile to cross the blood-brain barrier. Based on its physicochemical properties (logP[octanol/water] = 1.09), the compound may significantly cross the BBB, but may perhaps attain concentrations lower in the brain than those in blood. Additionally, no studies are available on the effect of allylnitrile on hippocampal neurogenesis. Although some authors have reported potential central nervous system (CNS) toxicity of allylnitrile (78) a thorough evaluation of the neuronal degeneration caused in the CNS of rats by several nitriles indicated no neuronal degeneration following allylnitrile except for incoming axons from the olfactory mucosa in the olfactory bulb. (40)

Spatial cognitive deficits and decreased hippocampal neurogenesis in the left hemisphere were observed 8 weeks after adult mice acquired profound SNHL and BV. Future research is needed to elucidate the isolated effect of SNHL versus BV on the hippocampus and to study long-term effects.

References

1. Liu L, Shen P, He T, et al. Noise induced hearing loss impairs spatial learning/memory and hippocampal neurogenesis in mice. Sci Rep 2016; 6: 20374. [Crossref]
2. Park SN, Kim MJ, Kim HL, Kong JS, Kim DK, Park SY. Cognitive dysfunction and degeneration with enhanced p-tau expression in the hippocampus of mice with noice-induced hearing loss 53rd Workshop on Inner Ear Biology, Montpellier.
3. Park SY, Kim MJ, Sikandaner H, Kim DK, Yeo SW, Park SN. A causal relationship between hearing loss and cognitive impairment. Acta Otolaryngol 2016; 136: 480-3. [Crossref]
4. Bronstein AM, Hood JD. Oscillopsia of peripheral vestibular origin. Central and cervical compensatory mechanisms. Acta Otolaryngol 1987; 104: 307-14. [Crossref]
5. Grunfeld EA, Morland AB, Bronstein AM, Gresty MA. Adaptation to oscillopsia: a psychophysical and questionnaire investigation. Brain 2000; 123 (Pt 2): 277-90. [Crossref]
6. Huygen PL, Verhagen WI, Theunissen EJ, Nicolasen MG. Compensation of total loss of vestibulo-ocular reflex by enhanced optokinetic response. Acta Otolaryngol Suppl 1989; 468: 359-64. [Crossref]
7. Zingler VC, Weintz E, Jahn K, et al. Follow-up of vestibular function in bilateral vestibulopathy. J Neurol Neurosurg Psychiatry 2008; 79: 284-8. [Crossref]
8. Hain TC, Cherchi M, Yacovino DA. Bilateral vestibular loss. Semin Neurol 2013; 33: 195-203. [Crossref]

9. De Belder J, Matthysen S, Claes AJ, Mertens G, Van de Heyning P, Van Rompaey V. Does otovestibular loss in the autosomal dominant disorder dfna9 have an impact of on cognition? a systematic review. Front Neurosci 2018; 11: 735. [Crossref]

10. Lucieer F, Duijn S, Van Rompaey V, et al. Full spectrum of reported symptoms of bilateral vestibulopathy needs further investigation-a systematic review. Front Neurol 2018; 9: 352. [Crossref]

11. Herssens N, Verbecque E, McCrum C, et al. A Systematic review on balance performance in patients with bilateral vestibulopathy. Phys Ther 2020; 100: 1582-94. [Crossref]

12. Previc FH, Krueger WW, Ross RA, Roman MA, Siegel G. The relationship between vestibular function and topographical memory in older adults. Front Integr Neurosci 2014; 8: 46. [Crossref]

13. Smith PF, Zheng Y, Horii A, Darlington CL. Does vestibular damage cause cognitive dysfunction in humans? J Vestib Res. 2005; 15: 1-9.

14. Lundin-Olsson L, Nyberg L, Gustafson Y. "Stops walking when talking" as a predictor of falls in elderly people. Lancet 1997; 349: 617. [Crossref]

15. Bessot N, Denise P, Toupet M, Van Nechel C, Chavoix C. Interference between walking and a cognitive task is increased in patients with bilateral vestibular loss. Gait Posture 2012; 36: 319-21. [Crossref]

16. Hill AJ, Best PJ. Effects of deafness and blindness on the spatial correlates of hippocampal unit activity in the rat. Exp Neurol 1981; 74: 204-17. [Crossref]

17. Rossier J, Haeberli C, Schenk F. Auditory cues support place navigation in rats when associated with a visual cue. Behav Brain Res 2000; 117: 209-14. [Crossref]

18. Harun A, Oh ES, Bigelow R, Agrawal, Y. Vestibular function testing in individuals with cognitive impairment: our experience with sixty participants. Clin Otolaryngol 2017; 42: 772-6. [Crossref]

19. Brandt T, Schautzer F, Hamilton, DA, et al. Vestibular loss causes hippocampal atrophy and impaired spatial memory in humans. Brain 2005; 128(Pt 11): 2732-41. [Crossref]

20. Kremmyda O, Hufner K, Flanagin VL, et al. Beyond dizziness: virtual navigation, spatial anxiety and hippocampal volume in bilateral vestibulopathy. Front Hum Neurosci 2016; 10: 139. [Crossref]

21. Popp P, Wulff M, Finke K, Ruhl M, Brandt T, Dieterich M. Cognitive deficits in patients with a chronic vestibular failure. J Neurol 2017; 264: 554-63. [Crossref]

22. Glasauer S, Amorim MA, Viaud-Delmon I, Berthoz A. Differential effects of labyrinthine dysfunction on distance and direction during blindfolded walking of a triangular path. Exp Brain Res 2002; 145: 489-97. [Crossref]

23. Gottlich M, Jandl NM, Sprenger A, et al. Hippocampal gray matter volume in bilateral vestibular failure. Hum Brain Mapp 2016; 37: 1998-2006. [Crossref]

24. Kraus KS, Mitra S, Jimenez Z, et al. Noise trauma impairs neurogenesis in the rat hippocampus. Neuroscience 2010; 167: 1216-26. [Crossref]

25. Kim JS, Jung J, Lee HJ, et al. Differences in immunoreactivities of Ki-67 and doublecortin in the adult hippocampus in three strains of mice. Acta Histochem 2009; 111: 150-6. [Crossref]

26. Delay J, Pichot P, Thuillier J, Marquiset JP. [Effect of aminodipropionitrile on motor behavior of the white mouse]. C R Seances Soc Biol Fil 1952; 146: 533-4.

27. Balbuena E, Llorens J. Behavioural disturbances and sensory pathology following allylnitrile exposure in rats. Brain Res 2001; 904: 298-306. [Crossref]

28. Tanii H. Hayashi M, Hashimoto K. Nitrile-induced behavioral abnormalities in mice. Neurotoxicol 1989; 10: 157-65.

29. Tanii H, Kurosaka Y, Hayashi M, Hashimoto K. Allylnitrile: a compound which induces long-term dyskinesia in mice following a single administration. Exp Neurol 1989; 103: 64-7. [Crossref]

30. Llorens J, Aguillo A, Rodriguez-Farre, E. Behavioral disturbances and vestibular pathology following crotonitrile exposure in rats. J Peripher Nerv Syst 1998; 3:189-96.

31. Llorens J, Rodriguez-Farre, E. Comparison of behavioral, vestibular, and axonal effects of subchronic IDPN in the rat. Neurotoxicol Teratol 1997; 19: 117-27. [Crossref]

32. Llorens J, Dememes D, Sans A. The behavioral syndrome caused by 3,3'-iminodipropionitrile and related nitriles in the rat is associated with degeneration of the vestibular sensory hair cells. Toxicol Appl Pharmacol 1993; 123: 199-210. [Crossref]

33. Seoane A, Dememes D, Llorens J. Relationship between insult intensity and mode of hair cell loss in the vestibular system of rats exposed to 3,3'-iminodipropionitrile. J Comp Neurol 2001; 439: 385-99. [Crossref]

34. Saldaña-Ruíz S, Boadas-Vaello P, Sedó-Cabezón L, Llorens J. Reduced systemic toxicity and preserved vestibular toxicity following co-treatment with nitriles and CYP2E1 inhibitors: a mouse model for hair cell loss. J Assoc Res Otolaryngol 2013; 14: 661-71. [Crossref]

35. Johnson KR, Tian C, Gagnon LH, Jiang H, Ding D, Salvi, R. Effects of Cdh23 single nucleotide substitutions on age-related hearing loss in C57BL/6 and 129S1/Sv mice and comparisons with congenic strains. Sci Rep 2017; 7: 44450. [Crossref]

36. Boadas-Vaello P, Sedo-Cabezon L, Verdu E, Llorens J. Strain and sex differences in the vestibular and systemic toxicity of 3,3'-iminodipropionitrile in Mice. Toxicol Sci 2017; 156: 109-22. [Crossref]

37. Chanas B, Wang H, Ghanayem BI. Differential metabolism of acrylonitrile to cyanide is responsible for the greater sensitivity of male vs female mice: role of CYP2E1 and epoxide hydrolases. Toxicol Appl Pharmacol 2003; 193: 293-302. [Crossref]

38. Arifin WN, Zahiruddin WM. Sample size calculation in animal studies using resource equation approach. Malays J Med Sci 2017; 24: 101-5. [Crossref]

39. Van den Eynde K, Missault S, Fransen E, et al. Hypolocomotive behaviour associated with increased microglia in a prenatal immune activation model with relevance to schizophrenia. Behav Brain Res 2014; 258: 179-86. [Crossref]

40. Boadas-Vaello P, Riera J Fau - Llorens, J, Llorens J. Behavioral and pathological effects in the rat define two groups of neurotoxic nitriles. Toxicol Sci 2005; 88: 456-66. [Crossref]

41. Saxon D, White G. Episodic vestibular disruption following ablation of the inferior olive in rats: behavioral correlates. Behav Brain Res 2006; 175: 128-38. [Crossref]

42. Vignaux G, Chabbert C, Gaboyard-Niay S, et al. Evaluation of the chemical model of vestibular lesions induced by arsanilate in rats. Toxicol Appl Pharmacol 2012; 258: 61-71. [Crossref]

43. Boadas-Vaello P, Jover E, Saldaña-Ruíz S, et al. Allylnitrile metabolism by CYP2E1 and other CYPs leads to distinct lethal and vestibulotoxic effects in the mouse. Toxicol Sci 2009; 107: 461-72. [Crossref]

44. Baumgart JP, Zhou ZY, Hara M, et al. Isoflurane inhibits synaptic vesicle exocytosis through reduced Ca2+ influx, not Ca2+-exocytosis coupling. Proc Natl Acad Sci USA. 2015; 112: 11959-64. [Crossref]

45. Bielefeld EC. Influence of dose and duration of isoflurane anesthesia on the auditory brainstem response in the rat. Int J Audiol 2014; 53: 250-8. [Crossref]

46. Cederholm JM, Froud KE, Wong AC, Ko M, Ryan AF, Housley GD. Differential actions of isoflurane and ketamine-based anaesthetics on cochlear function in the mouse. Hear Res 2012; 292: 71-9. [Crossref]

47. Ruebhausen MR, Brozoski TJ, Bauer CAA comparison of the effects of isoflurane and ketamine anesthesia on auditory brainstem response (ABR) thresholds in rats. Hear Res 2012; 287: 25-9. [Crossref]

48. Santarelli R, Arslan E, Carraro L, Conti G, Capello M, Plourde, G. Effects of isoflurane on the auditory brainstem responses and middle latency responses of rats. Acta Otolaryngol 2003; 123: 176-81. [Crossref]

49. Stronks HC, Aarts MC, Klis SF. Effects of isoflurane on auditory evoked potentials in the cochlea and brainstem of guinea pigs. Hear Res 2010; 260: 20-9. [Crossref]

50. Thiele N, Koppl C. Gas Anesthesia ımpairs peripheral auditory sensitivity in barn owls (Tyto alba). eNeuro 2018; 5: ENEU-RO.0140-18.2018. [Crossref]

51. Verdoodt D, Eens S, Van Dam D, et al. Effect of oral allylnitrile administration on cochlear functioning in mice following comparison of different anesthetics for hearing assessment. Front. Toxicol 2021; 3. [Crossref]

52. Kim JU, Ahn YS, Suh JK, Chung JW. Effect of isoflurane on the hearing in mice. Korean J Audiol 2012; 16: 14-7. [Crossref]

53. Zingler VC, Cnyrim C, Jahn, et al. Causative factors and epidemiology of bilateral vestibulopathy in 255 patients. Ann Neurol 2007; 61: 524-32. [Crossref]

54. Zingler VC, Weintz E, Jahn K, et al. Causative factors, epidemiology, and follow-up of bilateral vestibulopathy. Ann N Y Acad Sci 2009; 1164: 505-8. [Crossref]

55. Lin FR, Yaffe K, Xia J, et al. Hearing loss and cognitive decline in older adults. JAMA Intern Med 2013; 173: 293-9. [Crossref]

56. Lin FR, Metter EJ, O'Brien RJ, Resnick SM, Zonderman AB, Ferrucci L. Hearing loss and incident dementia. Arch Neurol 2011; 68: 214-20. [Crossref]

57. Gurgel RK, Ward PD, Schwartz S, Norton MC, Foster NL, Tschanz JT. Relationship of hearing loss and dementia: a prospective, population-based study. Otol Neurotol 2014; 35: 775-81. [Crossref]

58. Fulton SE, Lister JJ, Bush AL, Edwards JD, Andel R. Mechanisms of the hearing-cognition relationship. Semin Hear 2015; 36: 140-9. [Crossref]

59. Castiglione A, Benatti A, Girasoli L, et al. Cochlear implantation outcomes in older adults. Hearing, Balance and Communication 2015; 13: 86-8. [Crossref]

60. Qian ZJ, Chang PD, Moonis G, Lalwani AK. A novel method of quantifying brain atrophy associated with age-related hearing loss. Neuroimage Clin 2017; 16: 205-9. [Crossref]

61. Uchida Y, Nishita Y, Kato T, et al. Smaller hippocampal volume and degraded peripheral hearing among japanese community dwellers. Front Aging Neurosci 2018; 10: 319. [Crossref]

62. Lin FR, Ferrucci L, An Y, et al. Association of hearing impairment with brain volume changes in older adults. Neuroimage 2014; 90: 84-92. [Crossref]

63. Yu YF, Zhai F, Dai CF, Hu JJ. The relationship between age-related hearing loss and synaptic changes in the hippocampus of C57BL/6J mice. Exp Gerontol 2011; 46: 716-22. [Crossref]

64. Freemyer A, Neal C, Nelson-Brantley J, Staecker H, Durham D. Early onset region and cell specific alterations of doublecortin expression in the cns of animals with sound damage induced hearing loss. IBRO Rep 2019; 7: 129-40. [Crossref]

65. Hitier M, Zhang YF, Sato G, Besnard S, Zheng Y, Smith PF. The effects of selective electrical stimulation of the rat cochlea on hippocampal field potentials. Hear Res 2020; 395: 108023. [Crossref]

66. Barnes CA. Memory deficits associated with senescence: a neurophysiological and behavioral study in the rat. J Comp Physiol Psychol 1979; 93: 74-104. [Crossref]

67. Harrison FE, Hosseini AH, McDonald MP. Endogenous anxiety and stress responses in water maze and Barnes maze spatial memory tasks. Behav Brain Res 2009; 198: 247-51. [Crossref]

68. Agrawal Y, Smith PF, Rosenberg PB. Vestibular impairment, cognitive decline and Alzheimer's disease: balancing the evidence. Aging Ment Health 2020; 24: 705-8. [Crossref]

69. Dobbels B, Mertens G, Gilles A, et al. Cognitive function in acquired bilateral vestibulopathy: a cross-sectional study on cognition, hearing, and vestibular loss. PLoS One 2020; 13: 340. [Crossref]

70. Dobbels B, Petermans O, Boon B, Mertens G, Van de Heyning P, Van Rompaey V. Impact of bilateral vestibulopathy on spatial and nonspatial cognition: a systematic review. Ear Hear 2019; 40: 757-65. [Crossref]

71. Dobbels B, Mertens G, Gilles A, et al. The virtual morris water task in 64 patients with bilateral vestibulopathy. Front Neurol 2020; 11: 710. [Crossref]

72. Besnard S, Machado ML, Vignaux G, et al. Influence of vestibular input on spatial and nonspatial memory and on hippocampal NMDA receptors. Hippocampus 2012; 22: 814-26. [Crossref]

73. Zheng Y, Balabhadrapatruni S, Baek JH, et al. The effects of bilateral vestibular loss on hippocampal volume, neuronal number, and cell proliferation in rats. Front Neurol 2012; 3: 20. [Crossref]

74. Balabhadrapatruni S, Zheng Y, Napper R, Smith PF. Basal dendritic length is reduced in the rat hippocampus following bilateral vestibular deafferentation. Neurobiol Learn Mem 2016; 131: 56-60. [Crossref]

75. Shi F, Liu B, Zhou Y, Yu C, Jiang T. Hippocampal volume and asymmetry in mild cognitive impairment and Alzheimer's disease: meta-analyses of MRI studies. Hippocampus 2009; 19: 1055-64. [Crossref]

76. zu Eulenburg P, Stoeter P, Dieterich M. Voxel-based morphometry depicts central compensation after vestibular neuritis. Ann Neurol 2010; 68: 241-9. [Crossref]

77. Allgoewer A, Mayer B. Sample size estimation for pilot animal experiments by using a Markov Chain Monte Carlo approach. Altern Lab Anim 2017; 45: 83-90. [Crossref]

78. Zang XP, Tanii H, Kobayashi K, et al. Behavioral abnormalities and apoptotic changes in neurons in mice brain following a single administration of allylnitrile. Arch Toxicol 1999; 73: 22-32. [Crossref]